NASA Technical Memorandum 104566, Vol. 9

SeaWiFS Technical Report Series

Stanford B. Hooker, Editor
NASA Goddard Space Flight Center
Greenbelt, Maryland

Elaine R. Firestone and A. W. Indest, Technical Editors
General Sciences Corporation
Laurel, Maryland

Volume 9, The Simulated SeaWiFS Data Set, Version 1

Watson W. Gregg
NASA Goddard Space Flight Center
Greenbelt, Maryland

Frank C. Chen, Ahmed L. Mezaache,
Judy D. Chen, and Jeffrey A. Whiting
General Sciences Corporation
Laurel, Maryland

National Aeronautics and
Space Administration

Goddard Space Flight Center
Greenbelt, Maryland 20771

1993

ABSTRACT

Data system development activities for the Sea-viewing Wide Field-of-view Sensor (SeaWiFS) must begin well before the scheduled 1994 launch. To assist in these activities, it is essential to develop a simulated SeaWiFS data set as soon as possible. Realism is of paramount importance in this data set, including SeaWiFS spectral bands, orbital and scanning characteristics, and known data structures. Development of the simulated data set can assist in identification of problem areas that can be addressed and solved before the actual data are received. This paper describes the creation of the first version of the simulated SeaWiFS data set. The data set includes the spectral band, orbital, and scanning characteristics of the SeaWiFS sensor and SeaStar spacecraft. The information is output in the data structure as it is stored onboard. Thus, it is a level-0 data set which can be taken from start to finish through a prototype data system. The data set is complete and correct at the time of printing, although the values in the telemetry fields are left blank. The structure of the telemetry fields, however, is incorporated. Also, no account for clouds has been included. However, this version facilitates early prototyping activities by the SeaWiFS data system, providing a realistic data set to assess performance.

1. INTRODUCTION

The Sea-viewing Wide Field-of-view Sensor (SeaWiFS) is an ocean color sensor scheduled for launch in 1994. A follow-on to the highly successful Coastal Zone Color Scanner (CZCS) mission (1978–1986), SeaWiFS is intended to provide improved estimates of chlorophyll concentrations in the world's oceans.

The SeaWiFS mission will provide an unprecedented set of global ocean color data on a regular basis (every two days in the absence of clouds, about a week otherwise). The CZCS, a proof-of-concept mission, was able to produce a single global image in its nearly eight year lifetime. The volumes of data produced by an operational global ocean color sensor pose challenges for a data processing system that were not encountered by the CZCS system. Development and rigorous testing activities must begin well before launch to avoid the sorts of delays in data processing and distribution that plagued the CZCS mission.

To facilitate the development of the data system for processing SeaWiFS data, it is essential to develop a simulated SeaWiFS data set as soon as possible. This data set should incorporate the characteristics of the SeaWiFS sensor, including spectral bands and orbital and scanning characteristics, and should do so in a realistic manner to allow proper preparation for actual data processing. While many of the data characteristics, contents, and anomalies may not be known until just before launch, development of the simulated data set can assist in identification of problem areas that can be addressed and solved before a fuller understanding of the data is achieved.

This paper describes the details of the creation of the first version of the simulated SeaWiFS data set. The data set includes the spectral band, orbital, and scanning characteristics of the SeaWiFS sensor and SeaStar spacecraft. The information is output in the data structure as it is stored onboard. Thus, it is a level-0 data set which can be taken from start-to-finish through a prototype data system. The data set is complete and correct at the time of printing, although, the values in the telemetry fields are left blank (the structure of the telemetry fields is incorporated, however). Also, no account for clouds has been included.

CZCS pigment data and a variety of radiative transfer models were used to create realistic SeaWiFS total radiances. These total radiances were Earth-located using a SeaWiFS orbital model to provide SeaWiFS-like viewing and solar geometries.

2. BACKGROUND

The improvements of SeaWiFS over CZCS are largely expected due to the existence of four new spectral bands: one at 412 nm (to discern dissolved organic matter, or Gelbstoff), one at 490 nm (to enable better estimates of chlorophyll at high concentrations), and two in the near-infrared at 765 and 865 nm (to improve the determination of atmospheric aerosols). Thus, SeaWiFS contains eight spectral bands compared to the four used in CZCS processing (CZCS actually contained six bands, but two were not used). Table 1 shows a comparison of the SeaWiFS spectral bands to the CZCS bands.

In addition to different spectral bands, SeaWiFS is also in a different orbit than the CZCS and has different viewing geometries. A comparison between SeaWiFS orbital and sensor characteristics and those of the CZCS is summarized in Table 2.

Due to limited onboard data recorder space, SeaWiFS will be able to obtain global coverage only at reduced resolution (every fourth pixel along-track and along-scan). These data are called Global Area Coverage (GAC) data. High resolution data may be recorded in the remaining data recorder area. There is estimated to be about 20 minutes per day of high resolution Local Area Coverage

(LAC) data. The effort here is to create both types of data, in order to simulate a representative SeaWiFS data set.

Table 1. SeaWiFS spectral bands and center wavelengths, are shown with those of CZCS, for comparison. Wavelengths (λ) are in nm.

SeaWiFS		*CZCS*	
Band No.	λ	Band No.	λ
1	412	1	443
2	443	2	520
3	490	3	550
4	510	4	670
5	555	5	750[1]
6	670	6	13,500[2]
7	765		
8	865		

1. Intended for surface vegetation analyses only (Williams et al. 1985).
2. Data suspect after 1979 (Williams et al. 1985).

3. METHODS

In order to maximize the usefulness and realism of the simulated SeaWiFS data set, CZCS pigment data were chosen as the data source. The method for simulating SeaWiFS data involves creating both LAC and GAC data. Details of the method are described in the following, but a general overview here is helpful.

The basic equation of radiative transfer for ocean color assumes separability of the radiance contributions from atmospheric and oceanic components:

$$L_t(\lambda) = L_r(\lambda) + T(\lambda)L_g(\lambda) + L_a(\lambda) + T(\lambda)L_W(\lambda) \quad (1)$$

where L_t is the total radiance at the sensor, L_r is the Rayleigh radiance, L_g is the sun glint radiance, L_a is the aerosol radiance, L_W is the water-leaving radiance, and T is the total transmittance (direct plus diffuse) from the ocean through the atmosphere to the spacecraft. The variable of interest in the creation of simulated data is L_t, which is what the sensor actually detects. To obtain realistic values of L_t, with ranges and means observed in the real ocean, it is desirable to create it using representative values of the components. This process begins with the generation of L_W derived from CZCS pigment values, and adding atmospheric contributions from simulated SeaWiFS viewing and solar geometries.

For both LAC and GAC data, real CZCS images of pigments were selected. The pigment fields were used to create normalized water-leaving radiances, $L_{WN}(\lambda)$, at the eight SeaWiFS bands using a semi-analytic radiance model modified for SeaWiFS (Gordon et al. 1988a). Then, simulated SeaWiFS orbits were propagated through these simulated radiance fields to produce actual SeaWiFS viewing geometries. An arbitrary day was chosen (the vernal equinox) to produce solar geometry. Given these simulated solar and viewing geometries, a realistic atmosphere was added by including Rayleigh scattering, aerosol scattering and absorption, water vapor absorption, oxygen absorption, and sun glint reflectance. Radiance contributions of each were summed, and diffusely transmitted water-leaving radiance was added to produce simulated total radiance received by the sensor. Finally, data structures for telemetry were inserted and science data were formatted into 10-bit words to create level-0 data.

3.1 Normalized Water-Leaving Radiances

Creating normalized water-leaving radiances L_{WN} is the first step, because L_{WN} is independent of viewing and solar geometry. The method for creating L_{WN} is taken from Gordon et al. (1988a). According to this model,

$$L_{WN}(\lambda) = \frac{(1-\rho_n)(1-\rho_N)F_0(\lambda)R(0^-,\lambda)}{n^2Q\,[1-rR(0^-,\lambda)]} \quad (2)$$

where ρ_n is the Fresnel reflectance of the sea surface for normal incidence, ρ_N is a normalized mean value of surface reflectance for direct and diffuse irradiance for a flat sea, F_0 is the extraterrestrial irradiance corrected for Earth-sun distance, $R(0^-,\lambda)$ is the irradiance reflectance just below the sea surface, n is the index of refraction, Q is the irradiance-to-radiance ratio (equals π for totally diffuse radiance), and r is the water-air reflectance for totally diffuse irradiance.

From Fresnel's Law, ρ_n is known a priori (Jerlov 1976), ρ_N is estimated from Gordon et al. (1988a) at 0.043, n is taken to be 1.341 (Austin 1974), and r is taken to be 0.48 (Gordon et al. 1988a). The ratio $R(\lambda)/Q$ is wavelength dependent, and is taken from Gordon et al. (1988a) as:

$$\frac{R(\lambda)}{Q} = 0.110\,\frac{b_b(\lambda)}{K(\lambda)} \quad (3)$$

where $b_b(\lambda)$ is the spectral backscattering coefficient, and $K(\lambda)$ is the spectral attenuation coefficient. $K(\lambda)$ is determined from Baker and Smith (1982) as

$$K(\lambda) = K_W(\lambda) + K_c(\lambda) + K_g(\lambda) \quad (4)$$

where $K_W(\lambda)$ is the attenuation coefficient of pure seawater, $K_c(\lambda)$ is that for phytoplankton, and $K_g(\lambda)$ is that for Gelbstoff, or yellow substances.

Use of this model for a SeaWiFS simulation requires values for wavelength-dependent parameters be chosen for SeaWiFS bands. Values for the mean extraterrestrial irradiance F_0 were taken from Neckel and Labs (1984), and spectrally weighted over all of the SeaWiFS bandwidths assuming a full-width half-maximum (FWHM), Gaussian spectral response (Table 3). The values were corrected for Earth-sun distance following Gordon et al. (1983):

$$F_0(\lambda) = \overline{F}_0(\lambda)\left[1 + 0.0167\cos\frac{2\pi(D-3)}{365}\right]^2 \quad (5)$$

Table 2. Orbit and sensor characteristics for the SeaWiFS and the CZCS, shown for comparison.

Characteristic	*CZCS*	*SeaWiFS*
Altitude (km)	955	705
Period (minutes)	104.0	98.9
Inclination	99.28°	98.25°
Equator Crossing Time (local)	Noon	Noon
Node Type	Ascending	Descending
Scan Width	39.34°	58.3° (LAC); 45° (GAC)
Instantaneous Field of View (IFOV)	0.05°	0.09°
Ground IFOV at Nadir (km)	0.825	1.12
Pixels Along Scan	1,968	1,285 (LAC); 248 (GAC)
Scan Period (seconds)	0.134	0.667 (LAC); 1.5 (GAC)
Scan Plane Tilt	±20° in 2° steps	+20°, 0°, −20°
Scan Ground Coverage (km)	1,566	2,802 (LAC); 1,502 (GAC)
Maximum Spacecraft Zenith Angle	46.8°	70.8° (LAC); 51.7° (GAC)
Digitization (bits)	8	10

where $\overline{F}_0(\lambda)$ is the mean extraterrestrial irradiance and D is the sequential day of the year.

Table 3. Values for mean extraterrestrial irradiance $F_0(\lambda)$ (mW cm^{-2} μm^{-1}), $k_c(\lambda)$, $k'_c(\lambda)$, $b_W(\lambda)$ (m^{-1}), $A(\lambda)$ (m^{-1}), and $B(\lambda)$ used in the creation of the SeaWiFS simulated data set.

λ	F_0	k_c	k'_c	b_W	A	B
410	171.92	0.208	1.077	0.0067	0.00313	0.20401
443	189.05	0.175	1.001	0.0048	0.00300	0.21770
490	193.60	0.121	0.963	0.0031	0.00284	0.23674
510	188.41	0.103	1.006	0.0026	0.00346	0.34070
555	185.90	0.076	1.144	0.0019	0.00330	0.35666
670	152.82	0.137	1.463	0.0008	0.00238	0.29579
765	123.27	0.040	1.732	0.0005	0.00221	0.32081
865	100.34	0.010	1.732	0.0003	0.00206	0.34400

The values for $K_W(\lambda)$ were taken from Baker and Smith (1982), and again spectrally weighted FWHM assuming a Gaussian response (Table 3). $K_c(\lambda)$ was computed from Baker and Smith (1982):

$$K_c(\lambda) = k_c(\lambda)[chl.\ a] \exp\left[-k'_c(\lambda) \log_{10} \frac{[chl.\ a]}{C_{\text{ref}}}\right]^2 + 0.001[chl.\ a]^2 \quad (6)$$

where $[chl.\ a]$ is chlorophyll concentration, C_{ref} is a reference chlorophyll value (0.5), and $k_c(\lambda)$ and $k'_c(\lambda)$ are spectral fit coefficients and were spectrally weighted over the SeaWiFS bands (Table 3). For this simulation, $K_g(\lambda)$ was assumed to be zero.

The backscattering coefficient $b_b(\lambda)$ may be expressed using components similar to the $K(\lambda)$ formulation (4):

$$b_b(\lambda) = 0.5\, b_W(\lambda) + b_{bc}(\lambda) \quad (7)$$

where $b_W(\lambda)$ is the total scattering coefficient for pure seawater and $b_{bc}(\lambda)$ is the backscattering coefficient of phytoplankton. The coefficient 0.5 is the backscattering-to-total scattering ratio for pure seawater. The backscattering coefficient for plankton, $b_{bc}(\lambda)$, was determined from an empirical relationship developed by Gordon et al. (1988a)

$$b_{bc}(\lambda) = A(\lambda)[chl.\ a]^{B(\lambda)} \quad (8)$$

where, the coefficients $A(\lambda)$ and $B(\lambda)$ were computed for SeaWiFS bands as shown in Table 3. The only remaining unknown for the model, then, is $[chl.\ a]$, which was obtained from CZCS data.

3.2 Orbit Model

A simulated SeaWiFS orbit is required to obtain realistic viewing and solar geometries, which are then used to produce the atmospheric contribution to the total radiance detected by the sensor. The method used here is to propagate a SeaWiFS orbit over a field of CZCS pigment values, use the values to compute $L_{WN}(\lambda)$ for SeaWiFS bands, and use the simulated scan and tilt positions to determine the location of the pigment value in Earth coordinates (geocentric latitude and longitude). Given this information, the spacecraft and solar zenith and azimuth angles can be calculated and then used to simulate the radiative properties of an atmosphere. This section describes the orbit model employed, the equations to compute latitude and longitude, and the viewing and solar geometries.

The orbital model used assumes a circular orbit. Thus, the only parameters required to propagate a simulated orbit were inclination, altitude, and epoch (see Table 1 for SeaWiFS inclination and altitude). The epoch was chosen such that the first orbit crossed the equator on the descending node at the Greenwich Meridian at exactly noon local time.

In such a simple orbit model, the location of successive sub-satellite points (the point on the Earth where the projection of the satellite lies) is a simple function of the

previous sub-satellite point and the travel time between the two points. From spherical trigonometry,

$$\sin[\Psi_s(t-t_0)] = \cos\delta \sin[\Psi_s(t_0)] + \sin\delta \cos[\Psi_s(t_0)] \cos(i') \quad (9)$$

where Ψ_s is the sub-satellite latitude at times t_0 and $t-t_0$, δ is the great circle distance from $\Psi_s(t_0)$ to $\Psi_s(t-t_0)$, and i' is inclination $i-90°$. The great circle distance is known from

$$\delta = 360\frac{\Delta t}{P} \quad (10)$$

where P is the nodal period. The longitude difference, $\Delta\omega_s$, is calculated similarly:

$$\Delta\omega_s = \cos^{-1}\left[\frac{\cos\delta - \sin[\Psi_s(t-t_0)]\sin[\Psi_s(t_0)]}{\cos[\Psi_s(t-t_0)]\cos[\Psi_s(t_0)]}\right]. \quad (11)$$

The new longitude, ω, equals the old longitude ω_0 minus the longitude difference $\Delta\omega$ plus a correction for Earth rotation

$$\omega = \omega_0 - \Delta\omega + 0.004167t \quad (12)$$

where the coefficient 0.004167 is the rate of rotation ($^\circ\,s^{-1}$).

3.3 Navigation of Pixels

Given sub-satellite longitude and latitude, and the scan and tilt angles, the Earth position of any given pixel is calculable. First, one must calculate the great circle distance from the sub-satellite point to the pixel:

$$\delta = \theta - \theta_s' \quad (13)$$

where θ is the spacecraft zenith angle, and θ_s' is the scan angle θ_s modified by tilt. Given θ_s, θ_s' is computed by a simple pitch rotation in the direction of the tilt. The spacecraft zenith angle, θ, is computed directly from

$$\theta = \sin^{-1}\left[\frac{R_e + H_s}{R_e}\sin\theta_s'\right] \quad (14)$$

where R_e is the mean Earth radius (6371.2 km) and H_s is the spacecraft altitude (705 km).

The pixel latitude and longitude are determined from spherical trigonometry. For the latitude:

$$\Psi = \sin^{-1}[\sin\Psi_s\cos\delta + \cos\Psi_s\sin\delta\cos\eta] \quad (15)$$

where η is the bearing from the sub-satellite point to the pixel along the direction of motion of the satellite (either $270° + i'$ for the left-hand side of the scan facing north or $90° - i'$ for the right-hand side facing south).

The longitude difference, $\Delta\omega$, from the sub-satellite point to the pixel is determined by

$$\Delta\omega = \cos^{-1}\left[\frac{\cos\delta - \sin\Psi_s\sin\Psi}{\cos\Psi_s\cos\Psi}\right] \quad (16)$$

The pixel longitude is determined from $\Delta\omega$ by either adding to, or subtracting from, the sub-satellite longitude, depending on which side of the scan the pixel is on; if it is west of the sub-satellite point a subtraction is performed.

3.4 Viewing and Solar Geometries

Once the pixel has been navigated to Earth coordinates, computation of viewing geometry (spacecraft zenith and azimuth angles) is straightforward. In fact, the spacecraft zenith angle θ has already been found (14). This leaves the computation of the spacecraft azimuth angle, which is defined as the angle from the pixel to the sub-satellite point, measured counterclockwise from true north (at the pixel)

$$\Phi = \frac{\sin\Psi_s - \cos\delta\sin\Psi}{\sin\delta\cos\Psi} \quad (17)$$

where Φ is the spacecraft azimuth angle (the other terms are defined above).

The determination of the solar geometry requires additional information to the pixel location. Specifically, this additional information includes the solar declination latitude Ψ_d, equation of time T_e [both obtained using standard methods, e.g., Iqbal (1983)], and the Greenwich Mean Time (GMT). GMT is determined by

$$H_{\mathrm{GMT}} = t_{\mathrm{EC}} - \frac{\omega_e}{15} + t_e \quad (18)$$

where H_{GMT} is GMT in hours, t_{EC} is the equator crossing time (in local time, i.e., noon) ω_e is the equator crossing longitude, and t_e is the time difference to or from the most recent equator crossing to the present position (in hours).

Given this information, plus the pixel location, the solar zenith angle θ_0 is computed from

$$\cos\theta_0 = \sin\Psi\sin\Psi_d + \cos\Psi\cos\Psi_d\cos\Omega \quad (19)$$

where Ω is the solar hour angle, computed from

$$\Omega = (H-12)15 + \omega + T_e. \quad (20)$$

The solar azimuth angle Φ_0 is computed by

$$\Phi_0 = \cos^{-1}\left[\frac{\sin\Psi_d - \sin\Psi\cos\theta_0}{\cos\Psi\sin\theta_0}\right] \quad (21)$$

The viewing geometries θ and Φ and solar geometries θ_0 and Φ_0 are now known and attention may be focused on the addition of an atmosphere.

3.5 Atmospheric Contributions

This section focuses on the computation of realistic atmospheric contributions to the total radiance, based on representative atmospheric conditions and the simulated

SeaWiFS viewing and solar geometries. This means determining the Rayleigh scattering, ozone absorption, water vapor absorption, oxygen absorption, aerosol scattering and absorption, and sun glint contributions. As a first step, absorption coefficients for the atmospheric gases must be determined and spectrally weighted over the SeaWiFS bands, as was done for the mean extraterrestrial irradiance. Absorption coefficients for ozone, water vapor, and oxygen (the spectral absorption characteristics of which all three fall to some extent within some SeaWiFS bandwidths) are shown in Table 4, along with the Rayleigh optical thickness for the SeaWiFS bands.

Table 4. Spectrally weighted (FWHM) Rayleigh optical thickness (τ_r), ozone absorption coefficient (a_{oz}), water vapor absorption coefficient (a_{wv}), and oxygen absorption coefficient (a_{ox}). Wavelengths, λ, are in nm. The units for the absorption coefficients are in cm^{-1}; τ_r is dimensionless.

λ	τ_r	a_{oz}	a_{wv}	a_{ox}
410	0.3191	0.0000	0.0000	0.0000
443	0.2364	0.0027	0.0000	0.0000
490	0.1562	0.0205	0.0000	0.0000
510	0.1326	0.0382	0.0000	0.0000
555	0.0938	0.0898	0.0000	0.0000
670	0.0437	0.0463	0.0006	0.0000
765	0.0255	0.0083	0.0000	6.9900
865	0.0155	0.0000	0.0008	0.0000

Following Gordon et al. (1983), the effects of the absorbing gases in the atmosphere were determined by assuming two trips of the extraterrestrial irradiance through the atmosphere. This was accomplished by

$$F_0' = F_0 T_{oz}(\theta_0) T_{oz}(\theta) T_{wv}(\theta_0) T_{wv}(\theta) T_{ox}(\theta_0) T_{ox}(\theta) \quad (22)$$

where wavelength dependence has been dropped and T represents the transmittance of the gaseous component in subscript. The θ_0 and θ dependencies represent the two paths through the atmosphere: θ_0 is the path from the sun to the Earth and θ is the path from the Earth to the satellite. The path lengths for each path are computed for water vapor and oxygen by (Kasten 1966):

$$M = \frac{1}{\cos\eta + 0.15(93.885 - \eta)^{-1.253}} \quad (23)$$

where η is θ_0 or θ.

The path length for ozone transmittance is slightly different due to the high altitude of ozone concentrations (Paltridge and Platt 1976):

$$M_{oz} = \frac{1.0035}{\cos^2\eta + 0.007^{-0.5}}. \quad (24)$$

These formulations avoid the assumption of a flat Earth.

The next step is to compute the Rayleigh scattering contribution L_r to the total radiance received at the satellite. Since multiple scattering Rayleigh tables are not yet available for SeaWiFS bands, the tables for the CZCS bands are used (Gordon et al. 1988b). There are two coincident bands for SeaWiFS and the CZCS (see Table 1): one at 443 nm and the other at 670 nm. The CZCS multiple scattering Rayleigh tables are used for these two bands. Values for non-coincident SeaWiFS bands are derived assuming a λ^{-4} principle. For bands 1–5 (412–555 nm), the procedure is as follows. Let $\lambda = 443$ nm; then,

$$x = I(\lambda)\lambda^4. \quad (25)$$

Now, for $\lambda = 412$ and 555

$$I(\lambda) = x\lambda^{-4} \quad (26)$$

from which the Rayleigh scattering is derived:

$$L_r(\lambda) = I(\lambda)F_0'(\lambda) \quad (27)$$

where $I(\lambda)$ is the Rayleigh intensity taken from the CZCS multiple scattering tables (Gordon et al. 1988b).

The procedure is similar for bands 6–8 (670–865 nm), except 670 is substituted for λ in (25), and 670 and 865 replace 412 and 555 in (26). When this method is applied to the CZCS bands at 520 and 550 nm, a maximum error of 3.2% is obtained for $\theta_0 = 60$ and $\theta = 50$. The error is less at all smaller angles tested.

Next, the aerosol radiances, L_a, must be determined. According to Gordon and Castaño (1989) the aerosol radiance is determined by

$$L_a = \frac{\omega_a \tau_a p_a F_0' M}{4\pi} \quad (28)$$

where ω_a is the single scattering albedo of the aerosol, τ_a is the optical thickness, and p_a is a factor to account for the probability of scattering to the spacecraft for three different paths from the sun (Gordon and Castaño 1989). In (28) M has been substituted for Gordon and Castaño's (1989) $1/\cos\theta$ to allow calculations on a curved Earth.

The assumption is made that the aerosol obeys the Ångström formulation

$$\tau_a = \beta\lambda^{-\alpha} \quad (29)$$

and the Gregg and Carder (1990) model may be used to obtain β and α, as a function of wind speed. Wind speeds were obtained from six years of data from the Fleet Numerical Oceanography Center (FNOC), made available from the NASA Climate Data System (NCDS). The mean wind speeds over these six years at 2.5 × 2.5° spatial resolution were used.

The aerosol scattering albedo, ω_a, was also computed using Gregg and Carder (1990). The factor p_a was computed from Gordon and Castaño (1989)

$$p_a = \frac{1}{4\pi}\left[P(\theta^-) + [\rho(\theta_0)+\rho(\theta)]\,P(\theta^+)\right] \quad (30)$$

where $\rho(\theta_0)$ and $\rho(\theta)$ are the Fresnel reflectances for solar and viewing geometries, respectively, and P is the aerosol scattering phase function for the forward scattering angles $P(\theta^+)$, i.e., scattering toward the surface and reflected off the ocean or reflected first and then scattered toward the spacecraft, and backward angles $P(\theta^-)$, i.e., backscattered from the atmosphere.

$P(\theta^\pm)$ is determined using a Henyey-Greenstein function for marine aerosols

$$P(\theta^\pm) = \frac{a(1-g_1^2)}{(1+g_1^2-2g_1\cos\theta^\pm)^{1.5}} + \frac{(1-a)(1-g_2^2)}{(1+g_2^2-2g_2\cos\theta^\pm)^{1.5}} \quad (31)$$

where $a = 0.983$, $g_1 = 0.82$, and $g_2 = -0.55$ (Gordon and Castaño 1989). As defined in Gordon and Castaño (1989):

$$\cos\theta^\pm = \pm\cos\theta_0\cos\theta - \sin\theta_0\sin\theta\cos(\Phi-\Phi_0). \quad (32)$$

The next contribution to be accounted for is that of sun glint radiance diffusely transmitted to the spacecraft (TL_g). Sun glint at the surface for a given viewing and solar geometry may be expressed by (Cox and Munk 1954):

$$L_g = \frac{\rho_n\,T_0(\lambda,\theta_0)\,F_0(\lambda)\,p_w(\theta,\Phi,\theta_0,\Phi_0,W)}{4\cos\theta\,\cos^4\theta_N} \quad (33)$$

where $p_w(\theta,\Phi,\theta_0,\Phi_0)$ is the probability of seeing sun glitter in the direction θ, Φ given the sun in position θ_0,Φ_0 as a function of wind speed (W), and θ_N is the angle with respect to nadir of the sea surface slopes to produce a reflection angle to the spacecraft (Viollier et al. 1980). The term $T_0(\lambda,\theta_0)$ represents the total downward transmittance of irradiance as a function of θ_0 and the absorbing gases in the atmosphere. It may be expressed as the sum of the direct and diffuse transmittances (again dropping wavelength dependence)

$$T_0(\theta_0) = t_d(\theta_0) + t_s(\theta_0) \quad (34)$$

where the subscripts d and s represent direct and diffuse components, respectively. The transmittance t_d is simply the transmittance after absorption by the gaseous components of the atmosphere, scattering and absorption by aerosols, and scattering by Rayleigh (dropping the angular dependence):

$$t_d = t_r\,t_{aa}\,t_{oz}\,t_{wv}\,t_{ox}. \quad (35)$$

Some of the scattered Rayleigh and aerosol components continues forward and contributes to the total irradiance at the surface. These are expressed separately as:

$$t_s = t_{oz}\,t_{wv}\,t_{ox}\,t_{aa}\left[\frac{1-t_r^{0.95}}{2} + t_r^{1.5}F_a(1-t_{as})\right] \quad (36)$$

where t_{aa} is the aerosol transmittance after absorption

$$t_{aa} = e^{-(1-\omega_a)\tau_a M} \quad (37)$$

and t_{as} is analogously the transmittance after scattering (Justus and Paris 1985)

$$t_{as} = e^{(-\omega_a\tau_a M)}. \quad (38)$$

In (36)–(38), F_a is the forward scattering probability of the aerosol, taken from Bird and Riordan (1986), ω_a is the single scattering albedo of the aerosol, and τ_a is the aerosol optical thickness.

If $L_g(\lambda)$ is the sun glint radiance at the surface, $TL_g(\lambda)$ is that received by the sensor, where T is the total transmittance from the Earth to the satellite. It is defined in (34)–(38) with θ substituted for θ_0.

Finally, the normalized water-leaving radiance L_{WN} must be converted into the water-leaving radiance measured at the satellite TL_W. This is expressed by Gordon (1990) as

$$TL_W = L_{WN}(1-\rho)\,T_0\cos\theta_0. \quad (39)$$

The weighted direct plus diffuse reflectance, ρ, is computed as:

$$\rho = \rho_n W_d + \rho_N W_s \quad (40)$$

where W_d equals the direct irradiance divided by the total irradiance at the surface, and W_s is the diffuse irradiance divided by the total. These components are computed as a function of the atmospheric constituents and solar zenith angle using the model of Gregg and Carder (1990), as are the direct and diffuse reflectances, which are functions of the wind speed.

The simulated total radiance at the spacecraft, given in (1) is calculated by summing (27), (28), (33), and (39).

3.6 Atmospheric Conditions

There are five attenuating sources in the atmosphere that lie within SeaWiFS bands: Rayleigh scattering, ozone absorption, water vapor absorption, oxygen absorption, and aerosol scattering and absorption. Each was taken for the simulated data set at mean values. Rayleigh scattering and oxygen absorption are functions of atmospheric pressure for which a standard value of 1,013.25 mb was used. Ozone absorption was taken to be 340 Dobson units (DU) and absorption due to water vapor was assumed to be 1.5 cm.

Aerosols may be calculated as a function of visibility, a commonly reported meteorological parameter. Visibility was set to 15 km for the simulation, which corresponds to a mildly turbid atmosphere. Relative humidity (which determines, in part, the size distribution of the aerosols) was set at 80%. The 24-hour mean wind speed required for the aerosol model used by Gregg and Carder (1990), was estimated at 4.75 m s^{-1}, the global mean from 6 years of FNOC data, and the current wind speed, as noted before, was determined as the mean over 2.5° × 2.5° grid cells from the 6-year FNOC data set.

3.7 Ten-bit Words and Data Structures

The final step in developing a realistic SeaWiFS simulated data set is to convert the science data into 10-bit words and to structure the data fields according to the expected format for the downlink data. Not all of the telemetry fields have been decided upon, but the purpose here is to create as reasonable a data structure as possible to allow data system testing. Further developments can be incorporated as they are made.

Fig. 1 shows the preliminary stored data structures for LAC and GAC data. Depicted are the structures for a major frame of GAC and a major frame of LAC, each consisting of 3 minor frames. A major frame of GAC thus consists of 15 GAC scan lines, while a major frame of LAC consists of 3 LAC scan lines. The number of bytes in each minor frame is also denoted.

A single LAC scan line of SeaWiFS data contains 1,288 pixels, comprising 1,285 science pixels, a start synchronization pixel (also a 10-bit word) preceding the first pixel, a stop synchronization pixel at the end of the scan line, followed by a time delay integration (TDI) pixel. A GAC scan likewise contains 251 pixels, with 248 actual data pixels and three others in the same format as the LAC data. This representation is included in the simulated data set.

SeaWiFS simulated total radiance data were packed into 10-bit words according to

$$DC_{10}(\lambda) = \frac{L_t(\lambda) - L_{\mathrm{NER}}(\lambda)}{s(\lambda)}, \qquad (41)$$

where DC_{10} is the digital counts at 10-bit digitization, $L_{\mathrm{NER}}(\lambda)$ is the noise equivalent radiance (NER), or the minimum detectable radiance, and s is the slope for the range 0–1,023, which is applicable for 10-bit digitization, given by

$$s(\lambda) = \frac{L_{\mathrm{sat}}(\lambda) - L_{\mathrm{NER}}(\lambda)}{1{,}023} \qquad (42)$$

where $L_{\mathrm{sat}}(\lambda)$ is the saturation radiance for the sensor as a function of wavelength. $L_{\mathrm{NER}}(\lambda)$ and $L_{\mathrm{sat}}(\lambda)$ are shown in Table 5. This provides a realistic data set corresponding to the format stored on board the data recorder, and thus may be considered a level-0 data set.

Table 5. L_{NER} and saturation radiances (L_{sat}) for SeaWiFS (units are mW cm^{-2} μm^{-1} sr^{-1}).

Band	λ [nm]	L_{NER}	L_{sat}
1	412	0.0182	13.63
2	443	0.0125	13.25
3	490	0.0098	10.50
4	510	0.0088	9.08
5	555	0.0077	7.44
6	670	0.0056	4.20
7	765	0.0035	3.00
8	865	0.0023	2.13

4. APPLICATION OF CZCS DATA

The SeaWiFS GAC simulated data set was derived from the global CZCS data set (Feldman et al. 1989). This level-3 (remapped and gridded) data set was in dimensions of 2,048 × 1,024 (0.176° longitude by 0.176° latitude), and was cloud- and land-masked. The simulated SeaWiFS orbits passed through this CZCS pigment field in descending node (from north to south) for approximately 6.8 orbits to simulate a single data recorder dump of data. Start time for the simulation was the first contact at Wallops Flight Facility (WFF), the downlink station for SeaWiFS GAC data. Succeeding start times, as well as all stop times, were derived in previous simulations to maximize GAC coverage. The ultimate limit of the sensor was assumed to be 2 NER values, and the recorder was turned on whenever this limit was reached, subject to land features and ice cover. An 80% ice concentration was assumed as the limit for remote sensing purposes. Ice concentrations used were the minimum of six years of International Satellite Cloud Climatology Project (ISCCP) data, made available by NCDS. The start and stop times, in minutes travelled along the orbital track from equator crossing at ascending node, are given in Table 6.

The tilt was left at nadir pointing (0°) for this simulation to test the response of the data system to excessive sun glint. Normally, the sensor will be tilted aft when approaching the solar declination latitude from the north, and turned forward for the remainder of the descending node track; however, this strategy has yet to be finalized.

For the GAC simulation, no attempt was made to include clouds, and land features were masked (set to zero) as they occurred in the CZCS global data set.

The LAC simulation was initiated with the same global CZCS pigment data, using the same orbit trajectories, as will be the case for the real spacecraft. The sensor LAC recorder was turned on for three separate occasions, comprising one 3-minute scene and two 2-minute scenes, for a total of 7 minutes of LAC record time. This is about the correct amount of time left on the recorder after GAC data recording and some calibration activities. The start and stop times for the LAC recorder, and the associated simulated data set, are provided in Table 7. The difference between LAC and GAC data is the amount of data in a

SeaStar Stored Telemetry Format Definition

One-Sixth Second of Stored Stream (One Major Frame)

GAC Major Frame (MF):

mF	←6→	←2→	←4→	←620→	←44→	←44→	←188→	←2,016→	←2,016→	←2,016→	←2,016→	←2,016→	←2→	←100→	←1.2→
0	Frame Synch.	S/C ID	Time Tag	*S/C SOH TLM*	Inst. TLM	Cal. Table	Spare	Line n	Line $n+1$	Line $n+2$	Line $n+3$	Line $n+4$	Pad Pad	Aux. Synch.	Pad Pad
1	Frame Synch.	S/C ID	Time Tag	*S/C SOH TLM*	Inst. TLM	Cal. Table	Spare	Line $n+5$	Line $n+6$	Line $n+7$	Line $n+8$	Line $n+9$	Pad Pad	Aux. Synch.	Pad Pad
2	Frame Synch.	S/C ID	Time Tag	*S/C SOH TLM*	Inst. TLM	Cal. Table	Spare	Line $n+10$	Line $n+11$	Line $n+12$	Line $n+13$	Line $n+14$	Pad Pad	Aux. Synch.	Pad Pad
	←15→			←775→	←55→	←55→	←235→	←12,600→					←2.5→	←125→	←1.5→

LAC Major Frame (MF):

mF	←6→	←2→	←4→	←620→	←44→	←8→	←10,304→	←2→	←100→	←1.2→
0	Frame Synch.	S/C ID	Time Tag	*S/C SOH TLM*	Inst. TLM	Gain & TDI	Stored LAC Line	Pad Pad	Aux. Synch.	Pad Pad
1	Frame Synch.	S/C ID	Time Tag	*Historical SOH TLM*	Anc. TLM	Gain & TDI	Stored LAC Line	Pad Pad	Aux. Synch.	Pad Pad
2	Frame Synch.	S/C ID	Time Tag	*Sub-Packet or Fill Data*	Calib. Table	Gain & TDI	Stored LAC Line	Pad Pad	Aux. Synch.	Pad Pad
	←15→			←775→	←55→	←10→	←12,880→	←2.5→	←125→	←1.5→

Note: A minor frame (mF) is 11,091.2 10-bit words (13,864 bytes), there are 3 mFs per MF, and 6 MFs per second (triple the standard HRPT).

Fig. 1. Structure of the GAC and LAC data streams as stored on board. S/C indicates spacecraft, TLM means telemetry, and SOH means state of health. The number of words in each field is represented above the field, and the number of bytes in each field is represented underneath. The entries in *slanted typeface* are in an 8-bit telemetry format and the plain typeface entries are in a 10-bit format. (Courtesy of Steven Jackson, OSC.)

Table 6. Start and stop times (measured in minutes travelled along the orbit track from the equator crossing on ascending node), total time, start and stop latitudes, and solar zenith angles for the orbital simulations for the SeaWiFS simulated data set. The first contact with WFF is made on orbit 4 at 33.8743 min. and the second contact is on orbit 11 at night. Thus, the simulated data begins at 33.8743 min. and ends at the stop time of orbit number 10.

Day	Orbit	Times			Latitude		Solar Zenith	
	Number	Start	Stop	Total	Start	Stop	Start	Stop
80	1	27.0571	71.3008	44.243	78.285	-76.530	81.396	79.507
80	2	26.9876	69.2139	42.226	78.460	-69.996	81.648	71.923
80	3	26.9043	69.9826	43.078	78.670	-72.499	81.954	74.716
80	4	26.9154	70.7818	43.866	78.642	-74.995	81.910	77.621
80	5	27.7986	70.5321	42.733	76.235	-74.230	78.701	76.713
80	6	26.8932	71.6449	44.751	78.698	-77.496	81.991	80.757
80	7	26.9099	71.6449	44.735	78.656	-77.496	81.931	80.757
80	8	26.8932	69.2139	42.320	78.698	-69.996	81.991	71.923
80	9	30.3202	68.4647	38.144	68.207	-67.492	69.537	69.200
80	10	28.7511	68.4647	39.713	73.336	-67.492	75.239	69.200
80	11	27.8374	68.4647	40.627	76.121	-67.492	78.560	69.200
80	12	26.8932	68.4647	41.571	78.698	-67.492	81.991	69.200
80	13	26.9876	69.2139	42.226	78.460	-69.996	81.648	71.923
80	14	27.0571	69.2139	42.156	78.282	-69.996	81.396	71.923

LAC scan (Table 1), which is 1,285 pixels, with no gaps along-scan.

Table 7. Start and stop times (in minutes travelled along the orbit track from the equator crossing on ascending node) orbit numbers, and corresponding latitudes for the LAC simulation.

Orbit	Times			Latitude	
Number	Start	Stop	Total	Start	Stop
4	54.6	57.6	3.0	-18.35	-29.13
6	64.3	66.3	2.0	-53.03	-60.06
6	68.6	70.6	2.0	-67.95	-74.44

5. RESULTS AND DISCUSSION

Imagery of the simulated SeaWiFS total radiances $L_t(\lambda)$ for all 8 bands is shown in Figure 2 for GAC data. The start of the simulation was at the first visibility at WFF, which can be noted by the truncated orbit at the eastern edge of the image. Recall that for this simulation the sensor remained untilted, resulting in substantial sun glint influence near the equator (which is the solar declination for the vernal equinox, the time of the simulation). Tilting the sensor aft of the velocity vector when approaching the solar declination, and then forward when leaving would decrease the sun glint contribution to the total radiance substantially.

Note the decreases in $L_t(\lambda)$ toward the poles, due to a reduction in the flux of solar irradiance into the oceans, and the increases in $L_t(\lambda)$ at the scan edges, due to increased atmospheric contribution. The bands show progressively less total radiance from 412–865 nm. However, band 7 (765 nm) is the lowest because of large oxygen absorption (see Table 4). This absorption reduces the amount of saturation in the sun glint regions. Little evidence of water-leaving radiances is evident in most of the images. This is because the atmosphere dominates the total radiance over the oceans. Some evidence may be seen in the image of band 2 (443 nm), where the contribution of water-leaving radiance to the total is greatest under low chlorophyll concentrations.

The LAC recording areas are also depicted in Figs. 2–4. Note that they correspond with portions of the GAC orbits, but have a wider swath. Note also that the extra data across-track have very large $L_t(\lambda)$ values, due to increased atmospheric contribution as a function of the greater LAC spacecraft zenith angle at the edges.

This first version of the SeaWiFS simulated data set contains realistic total radiances, in a representative data record scenario: approximately 6.8 orbits of GAC data beginning at the first visibility of the downlink station at WFF, and 8 minutes of LAC record time, interspersed in the SeaWiFS orbits. Future improvements should incorporate representative values in the telemetry fields, accounting for clouds and land radiances. Also, a tilt strategy to minimize sun glint should be included. However, this version facilitates early prototyping activities by the SeaWiFS data system, providing a realistic data set to assess performance.

6. DATA AVAILABILITY

Version 1 of the simulated SeaWiFS data set is available from the authors on 9-track tape at 6,250 bits per inch (bpi). The tape is written using the VAX/VMS `BACKUP` command, on the assumption that most users have access

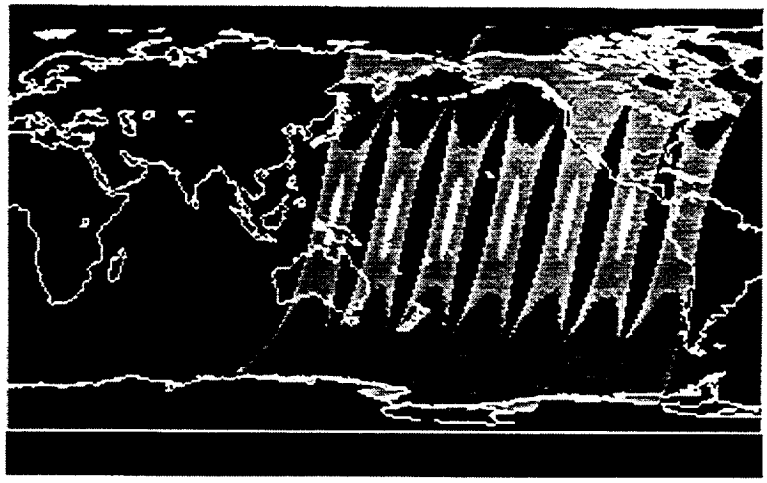

Band 1

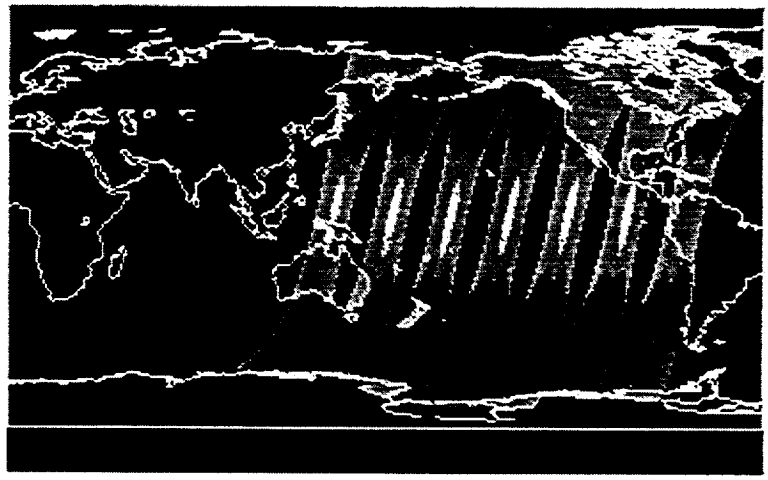

Band 2

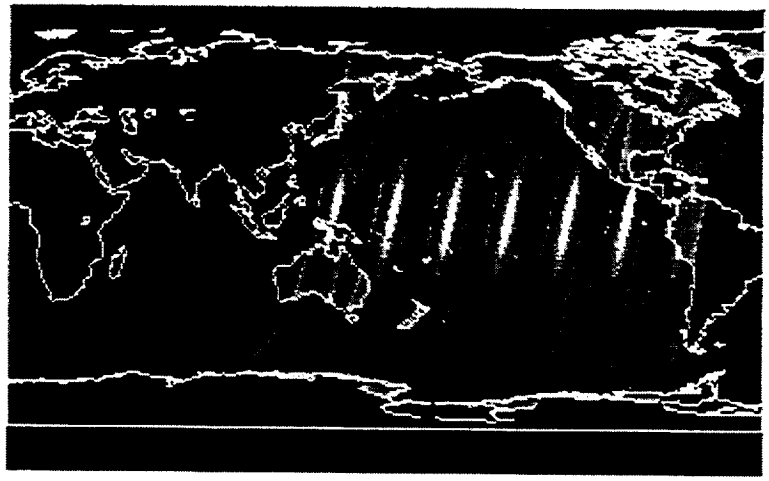

Band 3

Fig. 2. Simulated total radiances for GAC data for SeaWiFS bands 1–3.

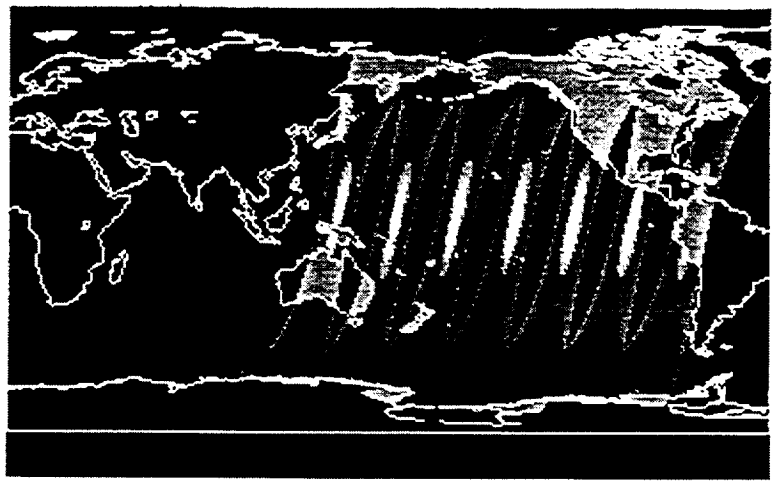

Band 4

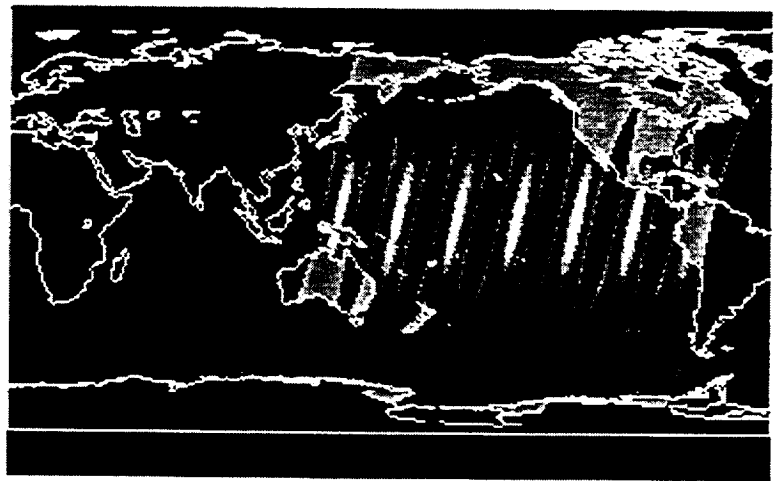

Band 5

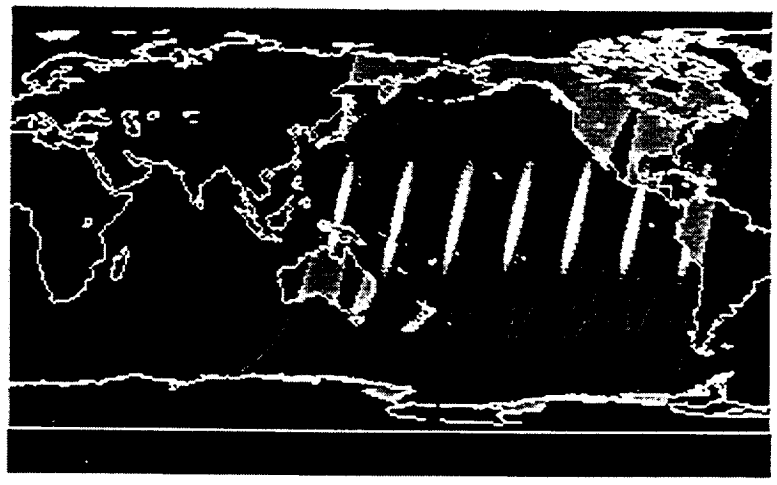

Band 6

Fig. 3. Simulated total radiances for GAC data for SeaWiFS bands 4–6.

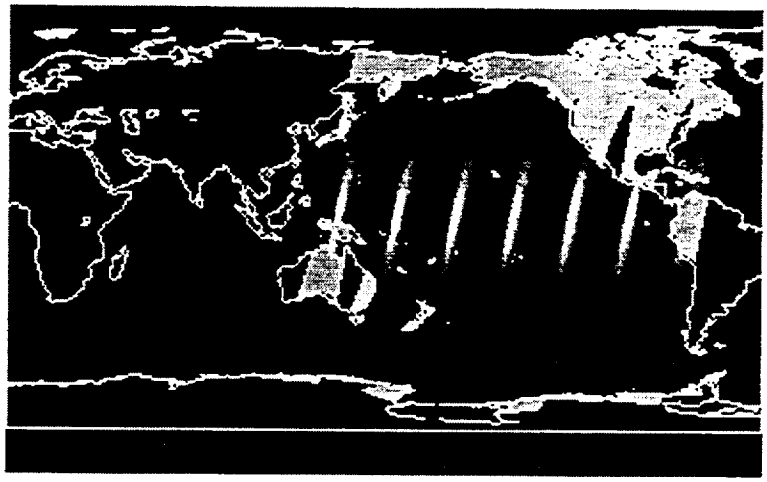

Band 7

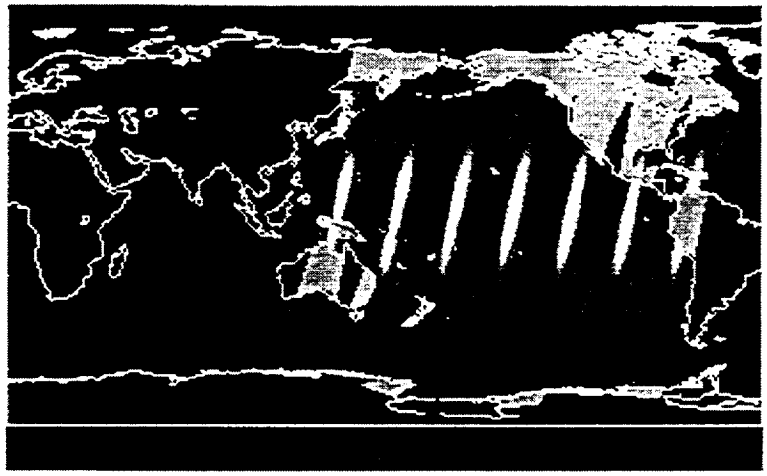

Band 8

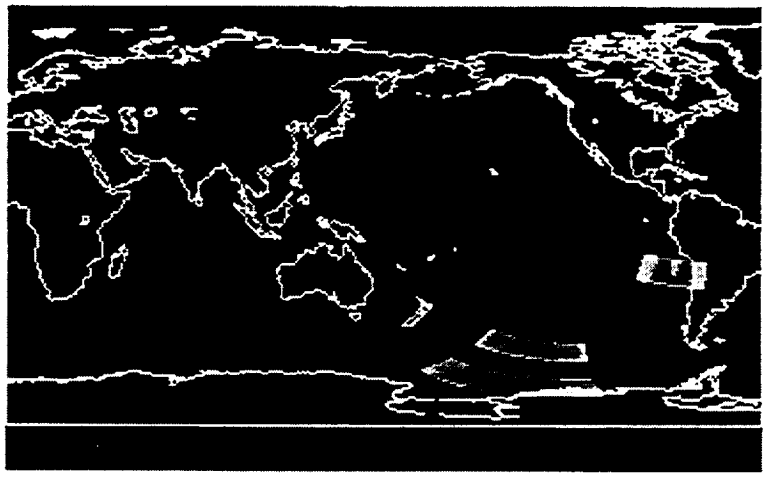

Band 2 LAC

Fig. 4. Simulated total radiances for GAC data for SeaWiFS bands 7-8, and LAC data for band 2.

to Digital Equipment Corporation (DEC) hardware. FORTRAN programs to read the data and strip out telemetry fields and science data are provided in the Appendices.

APPENDICES

A. Description
B. Program RGAC.FOR
C. Program RLAC.FOR
D. Program EXPAND.FOR
E. Program B2W.FOR

Appendix A

Description

The SeaWiFS simulated data sets and programs to read them are provided on a 6,250 bpi 9-track tape. The tape was generated using the VMS (version 5.4-3) BACKUP command and the following command sequence:

```
MOUNT/FOREIGN device
BACKUP/LOG device:simdat *.*/label=simdat/block=32256
DISMOUNT device
```

where device is the tape drive device name. (Note: 105 MBytes of free disk space are required to read the tape in its entirety.)

When the tape is loaded onto disk, 6 files are put in the current directory. GAC.DAT and LAC.DAT are the simulated data sets for GAC and LAC data, respectively. Listings of the source codes to read these data sets are provided in the following. This includes the main programs RGAC.FOR and RLAC.FOR and the two supporting subroutines, EXPAND.FOR and B2W.FOR. EXPAND.FOR is used to extract the minor frame data segments. B2W.FOR is used to unpack a 5-byte field into four 2-byte integers.

Appendix B

Program RGAC.FOR

```
program rgac
c
c  Program to read and sort simulated SeaWiFS GAC data.
c  by: Frank Chen, GSC.
c
implicit  none
character c(13864)
integer*2 s1(12)
character s2(775)
integer*2 s3(10458)
character s4(2)
c
c  Minor frame data structures
c
integer*2 FrameSync(6),SCID(2),TimeTag(4)
character SCSOH(775)
integer*2 InstTLM(44),CalTable(44),Spare(188)
integer*2 GAC(8,252,5)
integer*2 PAD1(2),AuxSync(100)
character PAD2(2)
c
c  Science data array
c
integer*2 ilt(8,248)
c
c  Total number of scan lines
c
integer*4 nscan
c
c  Minor frame number(1,2,3)
c
c integer*4 MinorFrameNo,msec_of_day, spacecraft_id
integer*2 day_of_year
integer*4 i,j,k
c
c  Orbit number, xlons, ylats, and gmt time(hr) for 5 GAC
c  scan lines within one minor frame. These fields are
c  temporary.
c
integer*4 iorb(5)
real*4    xlons(5),ylats(5),gmt(5)
c
c  Map the above fields within SCSOH
c
equivalence (iorb(1),SCSOH(197)), (xlons(1),SCSOH(217))
equivalence (ylats(1),SCSOH(237)), (gmt(1),SCSOH(257))
c
c  Map fields within minor frame to the three segments
c
equivalence (FrameSync(1),s1(1)), (SCID(1),s1(7))
equivalence (TimeTag(1),s1(9)), (SCSOH(1),s2(1))
equivalence (InstTLM(1),s3(1)), (CalTable(1),s3(45))
equivalence (Spare(1),s3(89)), (GAC(1,1,1),s3(277))
equivalence (PAD1(1),s3(10357)), (AuxSync(1),s3(10359))
equivalence (PAD2(1),s4(1))
c
100 format(i5,3f10.4)
200 format(8i5)
nscan = 0
c
open(4,file='gac.dat',status='old',form='unformatted')
20  continue
c
c   Read in one minor frame
c
read(4,end=999)c
c
c   Convert all 10-bit-word to 16-bit-word
c
call expand(c,s1,s2,s3,s4)
c
c  Calculate s/c id, minor fram number, day of year,
c  and msec of day
c
spacecraft_id = MOD(SCID(1)/8,16)
MinorFrameNo  = MOD(SCID(1)/128,4)
day_of_year   = TimeTag(1)/2
msec_of_day   = TimeTag(2)*1024.0*1024.0 +
*               TimeTag(3)*1024.0 + TimeTag(4)
do i=1,5
c
c  GAC(k,  1,i),k=1,8  80 bits GAC GainTDI
c  GAC(k,  2,i),k=1,8  80 bits GAC StartSync
c  GAC(k,  3,i),k=1,8  80 bits GAC DarkRestore
c  GAC(k,252,i),k=1,8  80 bits GAC StopSync
c
c  Check if the GAC data are valid
c
   if ((GAC(1,3,i).eq.0) .and. (GAC(2,3,i).eq.0) .and.
*     (GAC(3,3,i).eq.0) .and. (GAC(4,3,i).eq.0) .and.
*     (GAC(5,3,i).eq.0) .and. (GAC(6,3,i).eq.0) .and.
*     (GAC(7,3,i).eq.0) .and. (GAC(8,3,i).eq.0)) then
      write(6,*)' no more valid data'
      goto 999
   end if
   nscan = nscan + 1
   do j=4,251
      do k=1,8
         ilt(k,j-3)=GAC(k,j,i)
      end do
   end do
end do
goto 20
999 continue
```

```
close(4)
write(6,*)'Total no. of scan lines =',nscan
c
end
```

Appendix C

Program RLAC.FOR

```
program rlac
c
c  Program to read and sort SeaWiFS simulated LAC data.
c  by: Frank Chen, GSC.
c
implicit  none
character c(13864)
integer*2 s1(12)
character s2(775)
integer*2 s3(10458)
character s4(2)
c
c  Minor frame data structures
c
integer*2 FrameSync(6),SCID(2),TimeTag(4)
character SCSOH(775)
integer*2 InstTLM(44),LAC(8,1289)
integer*2 PAD1(2),AuxSync(100)
character PAD2(2)
c
c  History SCSOH and OX25 in minorframe 2,3
c
character HistSOH(775),OX25(775)
c
c  Ancilliary TLM and Calibration Table in minor
c  frame 2,3
c
integer*2 AncTLM(44),CalTable(44)
c
c  Science data array
c
integer*2 ilt(8,1285)
c
c  Total number of scan lines
c
integer*4 nscan
c
c  Minor frame number(1,2,3)
c
integer*4 MinorFrameNo,msec_of_day,spacecraft_id
integer*2 day_of_year
integer*4 i,j,k
c
c  Orbit number,xlons,ylats, and gmt time(hr) for LAC
c  scan  line within one minor frame. These fields
c  are temporary.
c
integer*4 iorb
real*4    xlons,ylats,gmt
c
c  Map the above fields within SCSOH
c
equivalence (iorb,SCSOH(197)), (xlons,SCSOH(217))
equivalence (ylats,  SCSOH(237)), (gmt,SCSOH(257))
c
c  Map fields within minor frame to the three segments
c
equivalence (FrameSync(1),s1(1)), (SCID(1),s1(7))
equivalence (TimeTag(1),s1(9)), (SCSOH(1),s2(1))
equivalence (InstTLM(1),s3(1)), (LAC(1,1),s3(45))
equivalence (PAD1(1),s3(10357)), (AuxSync(1),s3(10359))
equivalence (PAD2(1),s4(1)), (HistSOH(1),SCSOH(1))
equivalence (OX25(1),SCSOH(1)), (AncTLM(1),InstTLM(1))
equivalence (CalTable(1),InstTLM(1))
c
100 format(i5,3f10.4)
200 format(8i5)
nscan = 0
c
open(4,file='lac.dat',status='old',form='unformatted')
20 continue
c
c  Read in one minor frame
c
read(4,end=999)c
c
c  Convert all 10-bit-word to 16-bit-word
c
call expand(c,s1,s2,s3,s4)
c
c  Calculate s/c id, minor fram number, day of year,
c  and msec of day
c
spacecraft_id = MOD(SCID(1)/8,16)
MinorFrameNo  = MOD(SCID(1)/128,4)
day_of_year   = TimeTag(1)/2
msec_of_day   = TimeTag(2)*1024.0*1024.0 +
*               TimeTag(3)*1024.0 + TimeTag(4)
c
c  write(6,*)'day:',day_of_year,' scid:',
c  *      spacecraft_id,
c  *      ' frame:',MinorFrameNo
c
c  LAC(k,   1),k=1,8  80 bits LAC GainTDI
c  LAC(k,   2),k=1,8  80 bits LAC StartSync
c  LAC(k,   3),k=1,8  80 bits LAC DarkRestore
c  LAC(k,1289),k=1,8 <80 bits LAC StopSync
c
nscan = nscan + 1
do j=4,1288
   do k=1,8
      ilt(k,j-3)=LAC(k,j)
   end do
end do
goto 20
999 continue
close(4)
write(6,*)'Total no. of scan lines =',nscan
end
```

Appendix D

Program EXPAND.FOR

```
c This subroutine converts the input buffer (c) into
c four minor frame segments: s1, s2, s3, and s4.
c S1 consists  of 12 10-bit words containing the frame
c sync, the spacecraft id, and the time tag. S2
c is a the S/C SOH array.  S3 is the remainder 10458
c 10-bit words without the last  padding (1.5 bytes).
c S4 is the last padding.
c
subroutine expand(c,s1,s2,s3,s4)
implicit  none
character c(13864)
integer*2 s1(12)
character s2(775)
integer*2 s3(10458)
character s4(2)
character b(5)
integer*2 w(4)
integer*4 i,j,k
c
c  Process first I*2 segment
c
do i=0,11,4
   k = i*5/4
   do j=1,5
```

```
      b(j) = c(k+j)
   end do
   call b2w(b,w)
   do j=1,4
      s1(i+j) = w(j)
   end do
end do
c
c  Process second C*1 segment
c
k = 12*5/4
do i=1,775
   s2(i) = c(k+i)
end do
c
c  Process third I*2 segment
c
do i=0,10455,4
   k = (i+12)*5/4 + 775
   do j=1,5
      b(j) = c(k+j)
   end do
   call b2w(b,w)
   do j=1,4
      s3(i+j) = w(j)
   end do
end do
k = 13860
do j=1,3
   b(j) = c(k+j)
end do
b(4) = char(ichar(c(k+4)) .and. 240)
b(5) = char(0)
call b2w(b,w)
do j=1,3
   s3(10456+j) = w(j)
end do
s4(1) = char(MOD(ichar(c(13863)),16)*16 +
*       ichar(c(13864))/16)
s4(2) = char(MOD(ichar(c(13864)),16)*16)
return
end
```

Appendix E

Program B2W.FOR

```
c  Convert packed 5 bytes character(b) into four
c  two-byte-integer(w) each  contains 10-bit information.
c  MOD(n,2**m): modulus 'n' by '2**m'. extract lowest
c  'm' bits from the number 'n'.
c  n * (2**m): shift left  the number 'n' by 'm' bits.
c  n / (2**m): shift right the number 'n' by 'm' bits.
c
subroutine b2w(b,w)
implicit  none
character b(5)
integer*2 w(4)
integer*4 c(5)
integer*4 i
integer*4 p0 /1/, p2 /4/, p4 /16/, p6 /64/,
integer*4 p8 /256/
c
do i=1,5
   c(i) = ICHAR(b(i))
end do
w(1) = MOD(c(1),p8)*p2 + c(2)/p6
w(2) = MOD(c(2),p6)*p4 + c(3)/p4
w(3) = MOD(c(3),p4)*p6 + c(4)/p2
w(4) = MOD(c(4),p2)*p8 + c(5)/p0
return
end
```

Glossary

bpi	bits per inch
CZCS	Coastal Zone Color Scanner
DEC	Digital Equipment Corporation
DU	Dobson Units
FNOC	Fleet Numerical Oceanography Center
FORTRAN	Formula Translation (computer language)
FWHM	Full-Width Half-Maximum
GAC	Global Area Coverage
GMT	Greenwich Mean Time
IFOV	Instantaneous Field-of-View
ISCCP	International Satellite Cloud Climatology Project
LAC	Local Area Coverage
Level-0	Raw data.
Level-3	Gridded and averaged derived products.
MB	Megabytes
MF	Major Frame
mF	Minor Frame
NCDS	NASA Climate Data System
NER	Noise Equivalent Radiance
OSC	Orbital Sciences Corporation
SeaWiFS	Sea-viewing Wide Field-of-view Sensor
S/C	Spacecraft
SOH	State of Health
TDI	Time Delay Integration
TLM	Telemetry
VAX	Virtual Address Extension
VMS	Virtual Memory System
WFF	Wallops Flight Facility

Symbols

a	A constant equal to 0.983.
a_{ox}	Coefficient for oxygen absorption.
a_{oz}	Coefficient for ozone absorption.
a_{wv}	Coefficient for water vapor absorption.
$A(\lambda)$	Coefficient for calculating $b_b(\lambda)$.
$b_b(\lambda)$	Spectral backscattering coefficient.
$b_{bc}(\lambda)$	Spectral backscattering coefficient for phytoplankton.
$b_w(\lambda)$	Total scattering coefficient for pure seawater.
$B(\lambda)$	Coefficient for calculating $b_b(\lambda)$.
C_{ref}	Reference chlorophyll value (0.5).
$[chl.\ a]$	Chlorophyll concentration.
D	Sequential day of the year.
DC_{10}	Digital counts at 10-bit digitization.
$\overline{F}_0(\lambda)$	Mean extraterrestrial irradiance.
F_0	Extraterrestrial irradiance corrected for Earth-sun distance.
F_0'	Extraterrestrial irradiance corrected for the atmosphere.
F_a	Forward scattering probability of the aerosol.

g_1 A constant equal to 0.82.
g_2 A constant equal to -0.55.

H_{GMT} GMT in hours.
H_s Altitude of the spacecraft (for SeaStar 705 km).

i Inclination angle.
i' Inclination angle minus 90°.
I Rayleigh intensity.

$k_c(\lambda)$ Spectral fit coefficient weighted over the SeaWiFS bands.
$k'_c,(\lambda)$ Spectral fit coefficient weighted over the SeaWiFS bands.
$K(\lambda)$ Spectral attenuation coefficient.
$K_c(\lambda)$ Attenuation coefficients for phytoplankton.
$K_E(\lambda)$ Attenuation coefficient downwelled irradiance.
$K_g(\lambda)$ Attenuation coefficients for Gelbstoff.
$K_L(z,\lambda)$ Attenuation coefficient upwelled radiance .
$K_w(\lambda)$ Attenuation coefficients for pure seawater.

$L_a(\lambda)$ Aerosol radiance.
$L_g(\lambda)$ Sun glint radiance.
$L_{\mathrm{NER}}\lambda)$ Noise equivalent radiance.
$L_r(\lambda)$ Rayleigh radiance.
$L_{\mathrm{sat}}(\lambda)$ Saturation radiance for the sensor.
$L_t(\lambda)$ Total radiance at the sensor.
$L_u(z,\lambda)$ Upwelled spectral radiance.
$L_W(\lambda)$ Water-leaving radiance.
$L_{WN}(\lambda)$ Normalized water-leaving radiances leaving an ocean of given optical properties assuming no atmosphere and the sun directly overhead.

M Path length through the atmosphere.
M_{oz} Path length for ozone transmittance.

n Index of refraction.

Q Irradiance-to-radiance ratio (equals π for totally diffuse radiance).

p_a A factor to account for the probability of scattering to the spacecraft for three different paths from the sun.
p_w The probability of seeing sun glitter in the direction θ, Φ given the sun in position θ_0, Φ_0 as a function of wind speed (W).
P Nodal period.
P_a Probability of scattering to the spacecraft.
$P(\theta^+)$ Phase function for forward scattering.
$P(\theta^-)$ Phase function for backward scattering.

r Water-air reflectance for totally diffuse irradiance.
$R(0^-,\lambda)$ Irradiance reflectance just below the sea surface.
R_e Mean Earth radius (6371.2 km).

$s(\lambda)$ Slope for the range 0–1,023.

t Time variable.
t_0 Initial time.
t_{aa} Aerosol transmittance after absorption.
t_{as} Aerosol transmittance after scattering.
t_d Direct component of transmittance after absorption by the gaseous components of the atmosphere, scattering and absorption by aerosols, and scattering by Rayleigh.
t_e Time difference in hours between present position and most recent equator crossing.
t_{EC} Equator crossing time.
t_{oz} Transmittance after absorption by ozone.
t_r Transmittance after Rayleigh scattering.
t_s Diffuse component of transmittance after absorption by the gaseous components of the atmosphere, scattering and absorption by aerosols, and scattering by Rayleigh.
t_{wv} Transmittance after absorption by water vapor.
$T(\lambda,\theta)$ Total transmittance (direct plus diffuse) from the ocean through the atmosphere to the spacecraft along the path determined by the spacecraft zenith angle θ.
$T(\lambda,\theta)L_W(\lambda)$ The water-leaving radiance transmitted to the spacecraft.
$T_0(\lambda,\theta_0)$ Total downward transmittance of irradiance.
T_e Equation of time.
T_{ox} Transmittance of oxygen (O_2).
T_{oz} Transmittance of ozone (O_3).
$T_s(\lambda)$ Transmittance through the surface.
T_{wv} Transmittance of water vapor (H_2O).

W Wind speed.
W_d Direct irradiance divided by the total irradiance at the surface.
W_s Diffuse irradiance divided by the total irradiance.

α The power constant in the Ångström formulation.

β A constant in the Ångström formulation.

δ Great circle distance from $\Psi_s(t_0)$ to $\Psi_s(t-t_0)$.
Δt Time difference.
$\Delta\omega$ The longitude difference from the sub-satellite point to the pixel.
$\Delta\omega_s$ Longitude difference.

η Bearing from the sub-satellite point to the pixel along the direction of motion of the satellite.

λ Wavelength of light.

Ψ Pixel latitude.
Ψ_d Solar declination latitude.
$\Psi_s(t)$ Sub-satellite latitude as a function of time.

Φ Spacecraft azimuth angle.
Φ_0 Solar azimuth angle.

ρ Weighted direct plus diffuse reflectance.
$\rho(\theta)$ Fresnel reflectance for viewing geometry.
$\rho(\theta_0)$ Fresnel reflectance for solar geometry.
ρ_n Sea surface reflectance for direct irradiance at normal incidence for a flat sea.
ρ_N Reflectance for diffuse irradiance.

θ Spacecraft zenith angle.
θ_0 Solar zenith angle.
θ_N The angle with respect to nadir that the sea surface slopes to produce a reflection angle to the spacecraft.
θ_s Scan angle of sensor.
θ'_s Scan angle of sensor adjusted for tilt.

τ_a Aerosol optical thickness.
τ_r Rayleigh optical thickness.
$\tau_s(\lambda)$ Spectral solar atmospheric transmission.

ω Longitude variable.
ω_0 Old longitude value.
ω_a Single scattering albedo of the aerosol.
ω_e Equator crossing longitude.
ω_s Longitude variable.
Ω Solar hour angle.

References

Austin, R.W., 1974: The remote sensing of spectral radiance from below the ocean surface, In: *Optical Aspects of Oceanography,* N.G. Jerlov and E. Steemann-Nielsen, Eds., Academic Press, 317–344.

Baker, K.S., and R.C. Smith, 1982: Bio-optical classification and model of natural waters, 2. *Limnol. and Oceanography,* **27,** 500–509.

Bird, R.E., and C. Riordan, 1986: Simple solar spectral model for direct and diffuse irradiance on horizontal and tilted planes at the Earth's surface for cloudless atmospheres, *J. of Climate and Applied Meteorology,* **25,** 87–97.

Cox, C., and W. Munk, 1954: Measurement of the roughness of the sea surface from photographs of the sun's glitter, *J. Mar. Res.,* **44,** 838–850.

Feldman, G.C., N. Kuring, C. Ng, W. Esaias, C.R. McClain, J. Elrod, N. Maynard, D. Endres, R. Evans, J. Brown, S. Walsh, M. Carle, G. Podesta, 1989. Ocean Color: Availability of the global data set, *EOS, Transactions of the American Geophysical Union,* **70,** 634–635, 640–641.

Gordon, H.R., 1990. Radiometric considerations for ocean color remote sensors, *Applied Optics,* **29,** 3,228–3,236.

——, D.K. Clark, J.W. Brown, O.B. Brown, R.H. Evans, and W.W. Broenkow, 1983: Phytoplankton pigment concentrations in the Middle Atlantic Bight: Comparison of ship determinations and CZCS estimates, *Applied Optics,* **22,** 20–36.

——, O.B. Brown, R.H. Evans, J.W. Brown, R.C. Smith, K.S. Baker, and D.K. Clark, 1988a. A semianalytic radiance model of ocean color, *J. of Geophys. Res.,* **93,** 10,909–10,924.

——, J.W. Brown, and R.H. Evans, 1988b: Exact Rayleigh scattering calculations for use with the Nimbus-7 Coastal Zone Color Scanner, *Applied Optics, 27,* 862–871.

——, and D.J. Castaño, 1989: Aerosol analysis with Coastal Zone Color Scanner: A simple method for including multiple scattering effects, *Applied Optics,* **28,** 1,320–1,326.

Gregg, W.W., and K.L. Carder, 1990: A simple spectral solar irradiance model for cloudless maritime atmospheres, *Limnol. and Oceanography,* **35,** 1,657–1,675.

Iqbal, M., 1983: *An Introduction to Solar Radiation.* Academic Press, 390 pp.

Jerlov, N.G., 1976: *Marine optics,* Elsevier Scientific Publishing Co., New York, 231 pp.

Justus, C.G., and M.V. Paris, 1985: A model for solar spectral irradiance and radiance at the bottom and top of a cloudless atmosphere, *J. of Climate and Applied Meteorology,* **24,** 193–205.

Kasten, F., 1966: A new table and approximate formula for relative optical air mass, *Geophys. Biokimatol.,* **B14,** 206–223.

Neckel, H., and D. Labs, 1984: The solar radiation between 3300 and 12500 Å. *Solar Physics,* **90,** 205–258.

Paltridge, G.W., and C.M.R. Platt, 1976: Radiative processes in meteorology and climatology, *Developments in Atmospheric Science, Vol. 5.* Elsevier Scientific Publishing Co., New York, 318 pp.

Viollier, M., D. Tanre, and P.Y. Deschamps, 1980: An algorithm for remote sensing of water color from space,*Bound.-Layer Meteorology,* **18,** 247–267.

Williams, S.P., E.F. Szajna, and W.A. Hovis, 1985: Nimbus 7 Coastal Zone Color Scanner (CZCS) Level 1 data product users' guide, *NASA Technical Memorandum 86203,* 49 pp.

REPORT DOCUMENTATION PAGE

Form Approved
OMB No. 0704-0188

1. AGENCY USE ONLY *(Leave blank)*	2. REPORT DATE	3. REPORT TYPE AND DATES COVERED
	May 1993	Technical Memorandum

4. TITLE AND SUBTITLE
SeaWiFS Technical Report Series
Volume 9–The Simulated SeaWiFS Data Set, Version 1

5. FUNDING NUMBERS
970.2
NAS5-

6. AUTHOR(S)
Watson W. Gregg, Frank C. Chen, Ahmed L. Mezaache, Judy D. Chen, and Jeffrey A. Whiting
Editors: Stanford B. Hooker, Elaine R. Firestone, and A. W. Indest

7. PERFORMING ORGANIZATION NAME(S) AND ADDRESS(ES)
Laboratory for Hydrospheric Processes
Goddard Space Flight Center
Greenbelt, Maryland 20771

8. PERFORMING ORGANIZATION REPORT NUMBER
93B00086

9. SPONSORING/MONITORING AGENCY NAME(S) AND ADDRESS(ES)
National Aeronautics and Space Administration
Washington, D.C. 20546–0001

10. SPONSORING/MONITORING AGENCY REPORT NUMBER
TM–104566, Vol. 9

11. SUPPLEMENTARY NOTES
Frank C. Chen, Ahmed L. Mezaache, Judy D. Chen, Jeffrey A. Whiting, Elaine R. Firestone, and A. W. Indest: General Sciences Corporation, Laurel, Maryland.

12a. DISTRIBUTION/AVAILABILITY STATEMENT
Unclassified–Unlimited
Subject Category (48) leave blank
Report is available from the National Technical Information Service, U.S. Dept. of Commerce, 5285 Port Royal Road, Springfield, VA 22151; (703) 557–4650.

12b. DISTRIBUTION CODE

13. ABSTRACT *(Maximum 200 words)*

Data system development activities for the Sea–viewing Wide Field–of–view Sensor (SeaWiFS) must begin well before the scheduled 1994 launch. To assist in these activities, it is essential to develop a simulated SeaWiFS data set as soon as possible. Realism is of paramount importance in this data set, including SeaWiFS spectral bands, orbital and scanning characteristics, and known data structures. Development of the simulated data set can assist in identification of problem areas that can be addressed and solved before the actual data are received. This paper describes the creation of the first version of the simulated SeaWiFS data set. The data set includes the spectral band, orbital, and scanning characteristics of the SeaWiFS sensor and SeaStar spacecraft. The information is output in the data structure as it is stored onboard. Thus, it is a level–0 data set which can be taken from start to finish through a prototype data system. The data set is complete and correct at the time of printing, although the values in the telemetry fields are left blank. The structure of the telemetry fields, however, is incorporated. Also, no account for clouds has been included. However, this version facilitates early prototyping activities by the SeaWiFS data system, providing a realistic data set to assess performance.

14. SUBJECT TERMS
SeaWiFS, Oceanography, Data Set, Spectral Band, Orbital Characteristics, Scanning Characteristics

15. NUMBER OF PAGES
17

16. PRICE CODE

17. SECURITY CLASSIFICATION OF REPORT	18. SECURITY CLASSIFICATION OF THIS PAGE	19. SECURITY CLASSIFICATION OF ABSTRACT	20. LIMITATION OF ABSTRACT
Unclassified	Unclassified	Unclassified	Unlimited